Energetic behavior study of a direct solar dryer under different climate in Morocco

H. Samrani[a], A. Khyad[a], M.N. Bargach[a], R. Tadili[a] and A. Mcheqrane[b]

[a]Department of Physics, Laboratory of Solar Energy and Environment, Faculty of Sciences, Mohammed V University, B.P. 1014, Rabat, Morocco.
[b]Electrical Engineering Laboratory, Faculty of Science and Technology of Fez.
E-mail: hamidsamrani@yahoo.fr

Abstract

In this paper, we studied the variations of the incident and /or transmitted energy, received by a direct solar dryer (DSD), as well as the influence of dryer's dimensions on these energies for different climates of Morocco. Our study focused on the influence of the site's climatic specificity and the dryer's shape on solar energy collected or transmitted through comparison between its performances for several geometries. For various periods of the year, three Moroccan sites were selected for this study: Rabat (Latitude 34°00'47" N, Longitude 6°49'57" W), Tetouan (Latitude 35°34'42" N, Longitude 5°22'06" W) and Fez (Latitude 34°03'10" N, Longitude 4°58'58" W). Analysis of the dryer geometry and season effect allowed us to consider geometric scenarios of the solar dryer, which has led us to find an optimal design able of receiving a maximum of daily solar energy.

Keywords: *Direct solar dryer, solar radiation, solar transmittance, dryer's geometry*

Nomenclature:

DSD :	*Direct solar dryer.*
E_i :	*Incident energy.*
$E_{standard}$:	*Energy of dryer's standard form.*
G :	*Energy gain.*
LSEE :	*Laboratory of Solar Energy and Environment.*
MADIE :	*Monthly average of daily incident energy.*
MADTE :	*Monthly average of daily transmitted energy.*

1. Introduction

For the study of the direct dryer's solar energy balance, the three main parameters which affect the transmitted energy inside this dryer are the dryer's geometry, the glazing's transmission coefficient and the site of installation. A parametric study of the cover's geometry of a reduced dimensions dryer prototype was carried out for the Rabat site during the summer 2012 period [1]. This study highlighted the impact of the direct solar dryer's geometry and the transmission coefficient of the glass on its energetic behavior, in particular with regard to incident and transmitted solar radiation inside the dryer [2]. As the spectral nature and the energy intensity of solar radiation at ground level are highly linked to the site of the installation, it would be appropriate to take into account, in any energetic study of a solar system, the spatial and temporal climatic particularities of the site.

It is within this context, and with the aim to examine the influence of the site's climatic specificity on the variation of the transmitted solar energy inside the dryer, that we have focused our study. For this reason, we used hourly data from one year of global solar radiation measurements, carried out, simultaneously, in each of three Moroccan sites [3]. These sites correspond to three different climates: Rabat (characterized by a coastal climate), Tetouan (characterized by a Mediterranean climate) and Fez (characterized by a continental climate). Furthermore, the effect of solar dryer geometry on the profile of intercepted daily solar energy variation was determined, during a year, for the three sites.

In this work, we propose to study the energetic behavior of a DSD. For this purpose, we used hourly measurements of horizontal global solar radiation, performed in Rabat by the Laboratory of

Solar Energy and Environment (LSEE) of the Faculty of Science, or provided by the Electrical Engineering Laboratory in Faculty of Science and Technology of Fez, and the National Directorate of Meteorology for Tetouan. A detailed formulation to accurately calculate the different solar flow intercepted by the dryer's glass coverage was used [1]. A parametric study involving the dryer's shape (geometry effect) will allow us to study the energetic behavior by comparing its performance, for the above mentioned three climates, and for different seasons of the year (seasonal effect). The analysis of these two effects will enable us to consider the geometric schemes of the solar dryer leading to an optimal shape able to capture a maximum of daily solar energy.

2. Materials and methods

2.1 The prototype solar dryer

The various intercepted solar flow by the dryer coverage were calculated for a prototype solar dryer with standard geometry, composed of five facades whose four glazed transparent sides with thickness of 6 mm and a north oriented opaque wall. A perspective view and dimensions of the used dryer are schematically shown in Figure 1, below [4, 5].

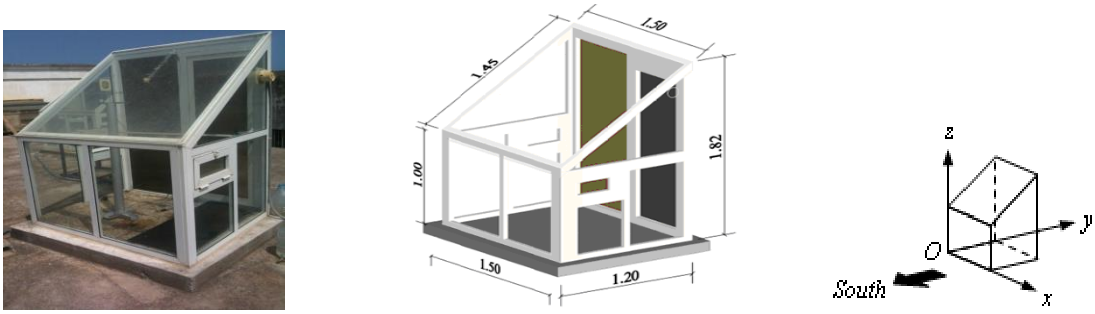

Figure 1-1 View in perspective and dimensions of the prototype dryer standard geometry.

This prototype solar dryer, installed in Laboratory of Solar Energy and Environment (LSEE), is equipped with the necessary measuring instruments, in particular: Pyranometers (used to measure global solar radiation), Anemometer (used to measure wind speed), Psychrometer (used to measure the relative humidity inside the dryer) and Thermocouples (used to measure temperature).

Hourly data of solar radiation are measured by meteorological stations which include acquisition chains, measuring instruments and sensors (used to measure exterior humidity) located outside in the air and on the ground. All measuring instruments and thermocouples are connected to this acquisition system which is controlled by a PC using a data acquisition program that provides the curves describing the variation and behavior of solar flow. The SUN program, developed in the LSEE Laboratory, allows calculating the solar radiation of all the dryer's facades on any day of the year.

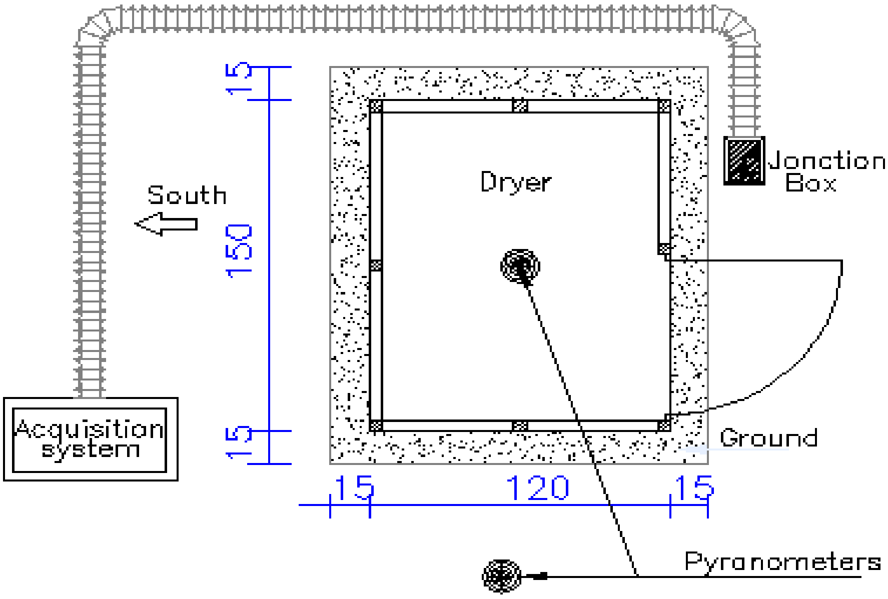

Figure 1-2 Plan view of the prototype dryer and equipment.

2.2 Measurements of daily solar energy for the three sites

Since the study of the dryer's energy balance requires the knowledge of the transmitted energy inside the dryer, and with the aim to control its energetic behaviour in response to the investigated site's climatic conditions, we used the hourly data of the global solar radiation incident on horizontal plane, simultaneously measured in the three sites during the year of 2013. Figure 2 shows the variation of the daily solar energy received by an horizontal plane for the three sites, Rabat, Tetouan and Fez.

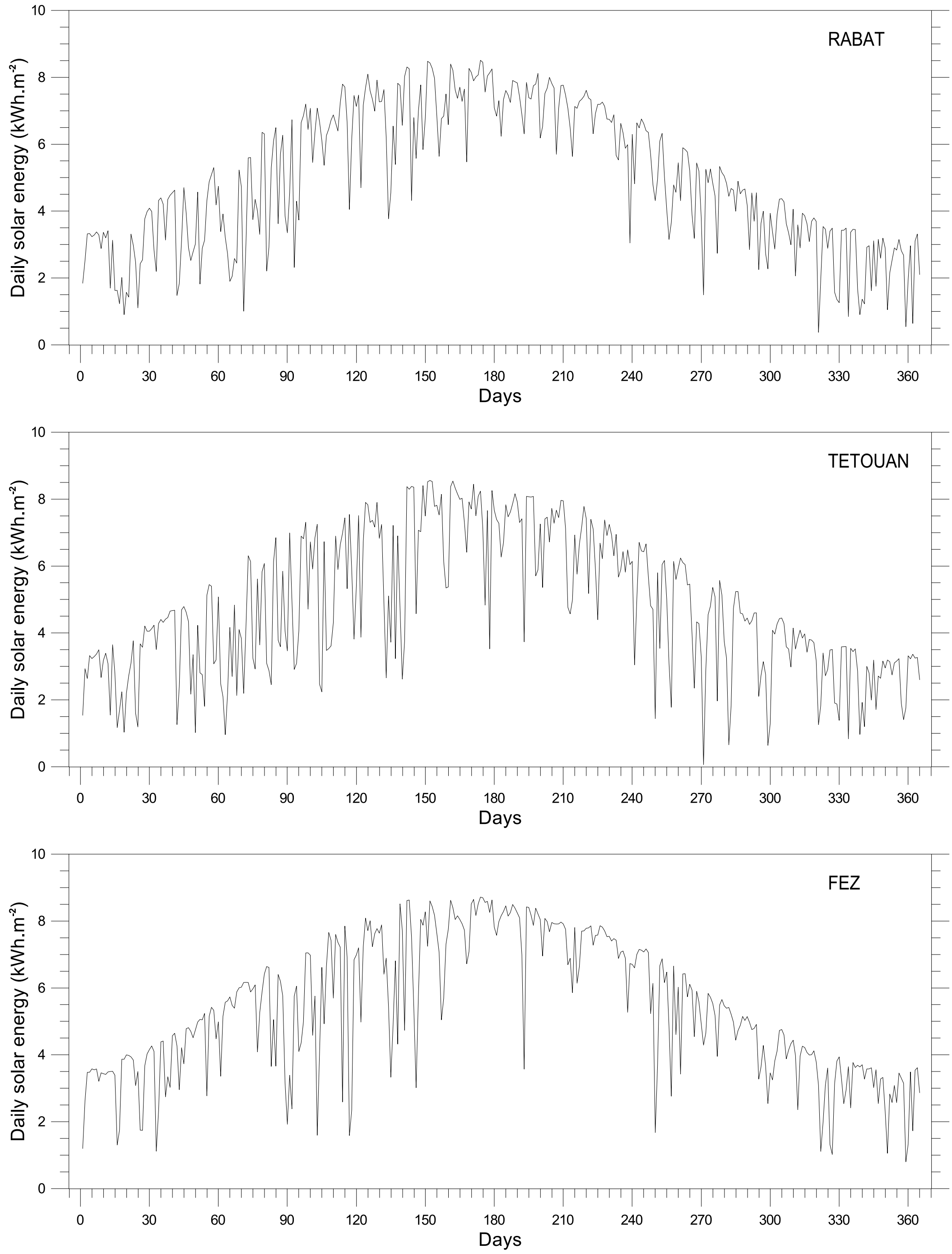

Figure 2 Variation of the daily solar energy for the three investigated sites of Rabat, Tetouan and Fez.

These figures allow us to note that the variation profiles of the annual global solar radiation are similar for the three sites, with specific occasional fluctuations for each site, presenting a maximum in summer period (8.50, 8.57, 8.71 kWh for Rabat, Tetouan and Fez, respectively) and a minimum in winter period (0.375, 0.068,0.800 kWh for Rabat, Tetouan and Fez, respectively).

2.3 Variations of the incident and transmitted energy by the dryer's standard form for different climates

2.3.1 Variations of the incident energy

Using the data measured during the year 2013, and by utilizing a software program developed in the laboratory LSEE, we have calculated the monthly average of the of daily incident energy (MADIE), by unit of coverage surface, for the dryer's standard geometry. A ponderation on all sides has allowed us to obtain the global solar radiation received by all the coverage [6,7,8]. Figure 3 represents the variation of the average MADIE for the three sites.

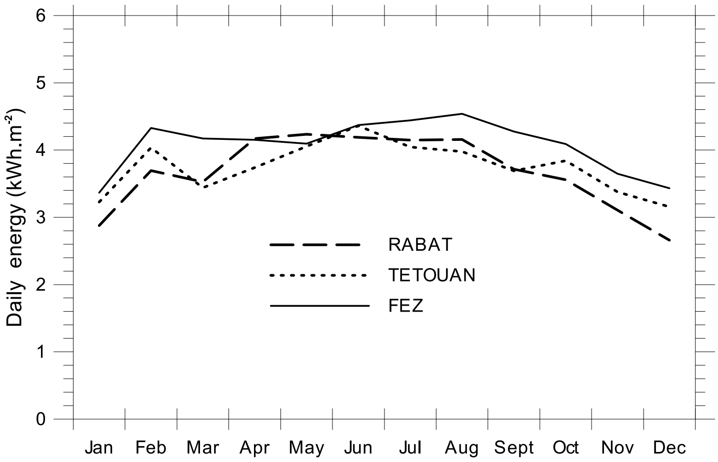

Figure 3 Variation of monthly average of daily incident energy (MADIE) for the three sites.

Table 1 presents the daily values of incident energy's monthly and yearly averages.

Sites	Daily energy (kWh.m^{-2}.Day^{-1})												
	Jan.	Feb.	March	Apr.	Mai	Jun.	Jul.	Aug.	Sep.	Oct.	Nov.	Dec.	**Average**
Rabat	2.88	3.69	3.53	4.17	4.23	4.19	4.15	4.16	3.72	3.56	3.11	2.66	**3.67**
Tetouan	3.23	4.04	3.44	3.74	4.05	4.36	4.05	3.98	3.69	3.84	3.38	3.16	**3.75**
Fez	3.37	4.33	4.17	4.15	4.10	4.37	4.44	4.54	4.28	4.09	3.65	3.43	**4.08**

Table 1: Monthly and yearly averages of the daily incident energy.

Figure 3 and Table 1 allow observing the following characteristics:

- the maximum daily energy received per unit of coverage surface has been achieved in May for the Rabat site (with a daily average of 3.67 kWh.m^{-2}.Day^{-1}), in June for the Tetouan site (with a daily average of 3.75 kWh.m^{-2}.Day^{-1}) and in August for the Fez site (with a daily average of 4.08 kWh.m^{-2}.Day^{-1});
- the daily energy exceeding the annual average for each site have been recorded during seven months in Rabat and Tetouan, and during nine months in Fez.

2.3.2 Variations of transmitted energy

Similarly, the transmitted solar energy by the coverage surface unit (standard geometry) was calculated [9,10]. Figure 4 illustrates the monthly average variation of this energy for the three sites. The values of these monthly averages are given in Table 2.

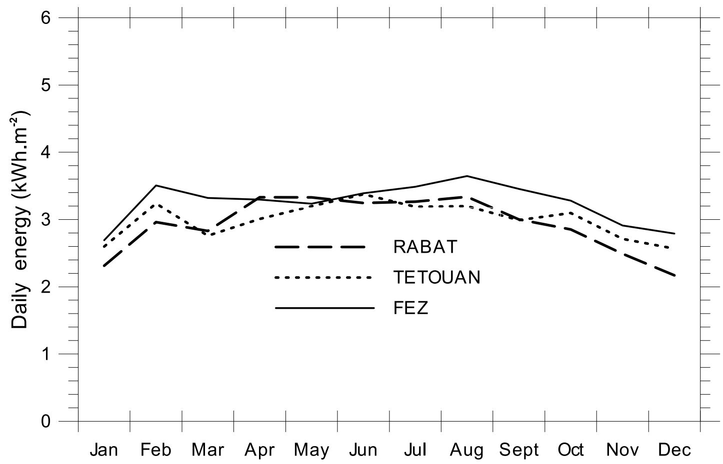

Figure 4 Variation of monthly average of daily transmitted energy (MADTE).

Table 2 Monthly and yearly averages of the daily transmitted energy.

Sites	Daily energy ($kWh.m^{-2}.Day^{-1}$)												
	Jan.	Feb.	March	Apr.	Mai	Jun.	Jul.	Aug.	Sep.	Oct.	Nov.	Dec.	**Average**
Rabat	2.31	2.96	2.83	3.33	3.33	3.25	3.27	3.32	3.00	2.85	2.49	2.17	**2.92**
Tetouan	2.60	3.24	2.76	3.01	3.20	3.38	3.19	3.20	2.99	3.10	2.71	2.57	**2.99**
Fez	2.69	3.51	3.32	3.30	3.24	3.39	3.49	3.65	3.46	3.28	2.91	2.79	**3.25**

Figure 4 and Table 2 show that:

- the maximum daily energy received per unit of coverage surface has been achieved in May for the Rabat Site (with a daily average of 2.92 $kWh.m^{-2}.Day^{-1)}$, in August for the site of Fez (with a daily average of 3.25 $kWh.m^{-2}.Day^{-1}$) and in June for the Tetouan site (with a daily average of 2.99 $kWh.m^{-2}.Day^{-1}$);
- daily energy exceeding the annual average has been registered during eight months in all sites.

Although, during a day, the transmission coefficient is not linear [1], comparison between figure 3 and figure 4 indicates that, during a year, for each site:

- periods of maximum intensities of both incident and transmitted energy coincide;
- the monthly average of daily transmission coefficient is practically constant (more than 0.776 in summer and less than 0.816 in winter).

Accordingly, the transmitted energy can be determined by a simple decreasing translation of incident energy. Therefore, it will be sufficient to examine the geometric shape variation impact on the incident global radiation variation profile and consequently the impact of the transmitted global radiation variation will be deducted equally.

3. Results and discussion

3.1 Impact of the DSD geometrical shape variation on the incident energy

After examining the incident energy variations effect's on the DSD standard form, the following results will present, for the three studied climates, the influence of the dryer dimensions changes on this energy.

For this purpose, we have associated the dryer to an orthogonal referential (O,x,y,z), whose axes are parallel to the three edges of the dryer, respectively (see Figure 1).

Through successive variations with regular step of 0.1 m, we have subsequently varied, from the standard form, one dimension of the dryer, the other dimensions remaining constant. The changes proposed are illustrated in Figure 5.

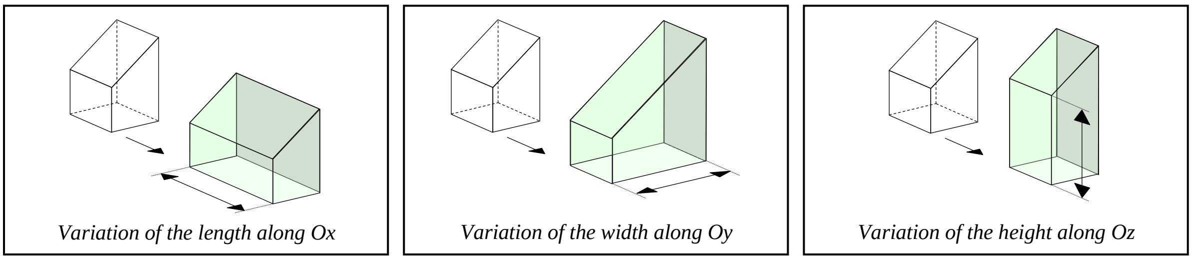

Figure 5 Scheme of changes along OX, OY and OZ.

3.1.1 Variation along the Ox direction

The dimensions of the dryer according to the Oy and Oz axes are equal to their standard values (1.2 m and 1.0 m, respectively), the variations are presented by figures 6 for X varying from 1.5 m to 16.0 m, by a step of 0.5 m (standard form presented in dotted lines).

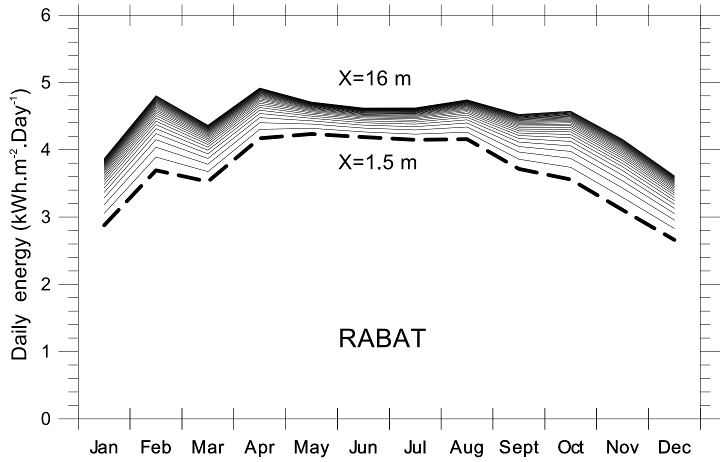

Figure 6-a

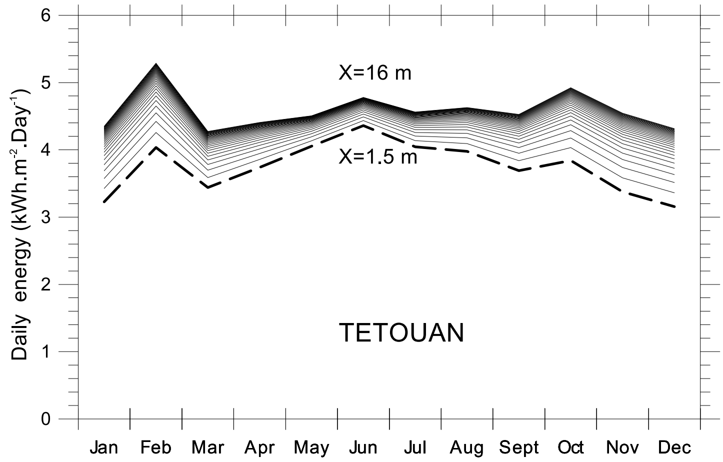

Figure 6-b

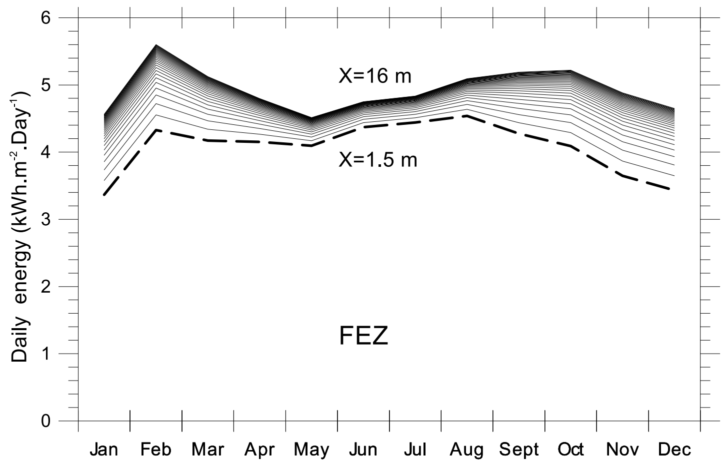

Figure 6-c

Figures 6 Variation of the MADIE average for different values of X.

These figures allow us to note that the augmentation of the X values promotes an increase of the MADIE average. The rate of this increase is, however, becoming less significant with the augmentation of X.

By defining the energy gain with the following report:

$$G_i = 100 \times \frac{E_i - E_{standard}}{E_{standard}} ,$$

Figure 7.a enables us to view the gain variation versus X for the three studied sites.

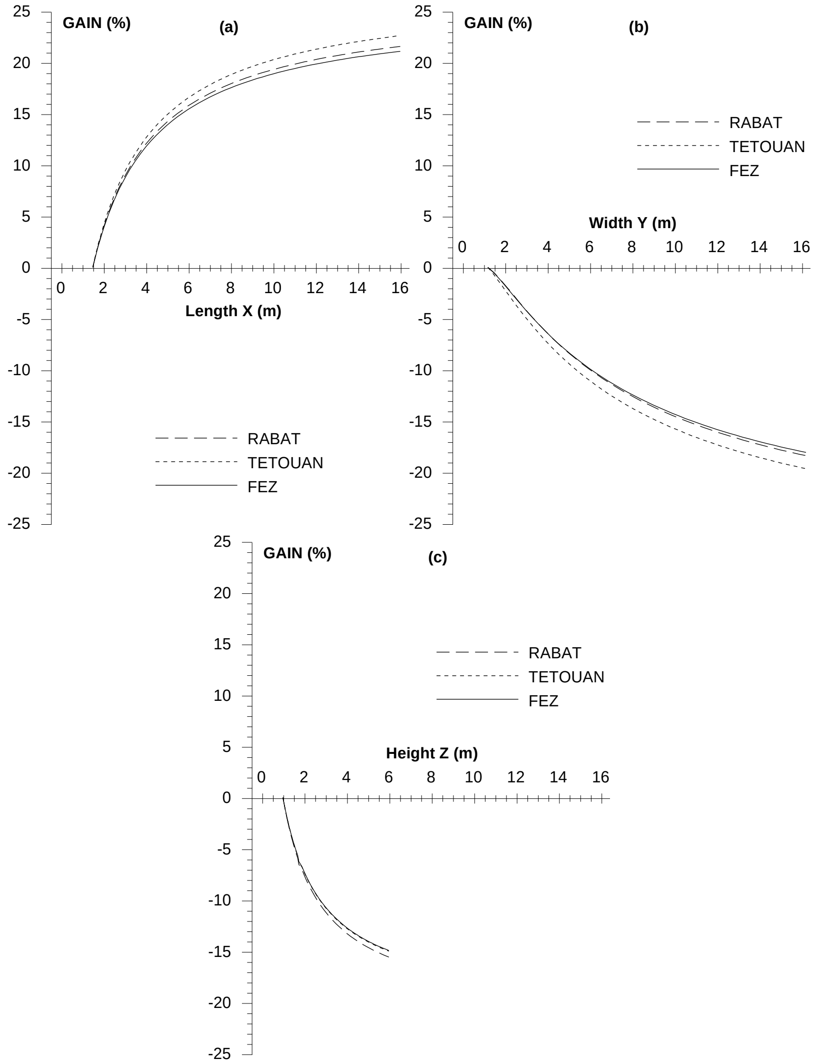

Figure 7 Evolution of the energy gain for the three sites.

From figure 7.a, it is observed that:

- the gain variation profile is similar for all the three sites;
- for high values of X and for the three sites under study, the gain increasing stabilizes at around a slightly different asymptotic maximum value for each site;
- the energy gain of the Tetouan site is substantially higher than that of Rabat and Fez.

3.1.2 Variation along the Oy direction

The dimensions of the dryer according to the Ox and Oz axes are equal to their standard values (1.5 m and 1.0 m, respectively), the variations are presented by figures 8 for Y varying from 1.2 m to 16.2 m, by a step of 0.6 m (standard form presented in dotted lines).

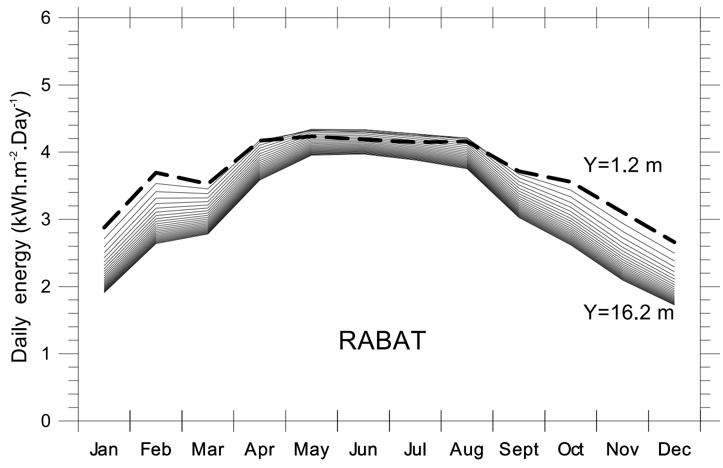

Figure 8-a

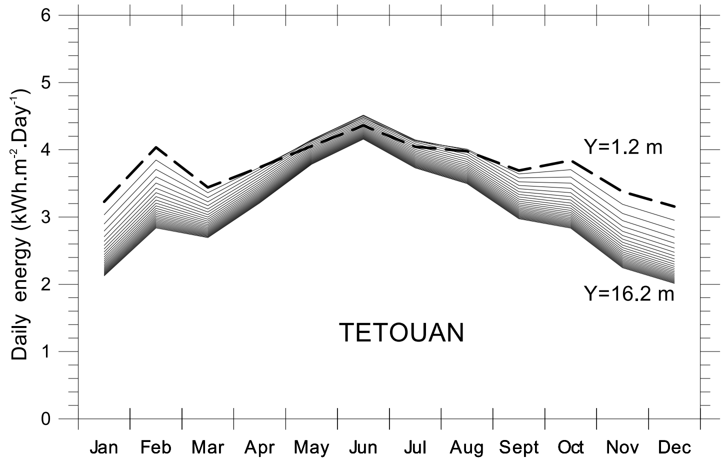

Figure 8-b

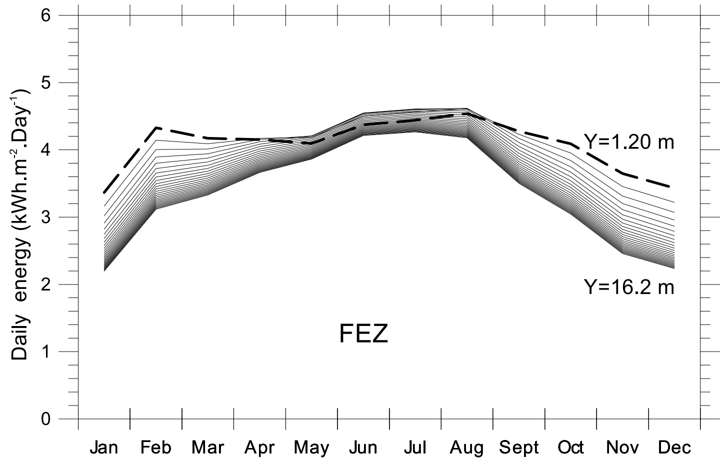

Figure 8-c

Figures 8 Variation of the MADIE average for different values of Y.

These figures show that, for the three studied sites and in the winter period, the increase of Y values leads to a decrease in the MADIE average's intensity compared to that received by the standard form. In summer period, the trend is the same except for some values of Y. This is due to the fact that since the intensity of radiation received by a slightly inclined surface is higher than that of a vertical surface, in summer season, the augmentation of Y values is accompanied by:

- a significant decline in the energy proportion received by the inclined surface;
- a slight increase in the energy proportion received by the vertical surfaces but not compensated by the inclined surface proportion which becomes predominant.

This leads to an overall decrease in the intensity of radiation, per surface unit, in the summer period and for some values of Y. Figure 7.b allows visualizing the variation of the gain as a function of Y for the three studied sites. From this figure, it is noted that:

- the gain variation profile is similar for all the three sites;
- the energy gain of the Tetouan site is substantially lower than of Rabat and Fez;
- in contrary to the variation in the Ox direction, in which the gain is increasing with X, the variation according to the Oy axis presents a negative gain, except for the four months of summer where it reverses and becomes positive for some values of Y, with a low magnitude not exceeding 2.5%.

3.1.3 Variation along the Oz direction

The dimensions of the dryer according to the Ox and Oy axes are equal to their standard values (1.5 m and 1.2 m, respectively), the variations are presented by figures 9 for Z varying from 1.0 m to 6.0 m, by a step of 0.1 m (standard form presented in dotted lines).

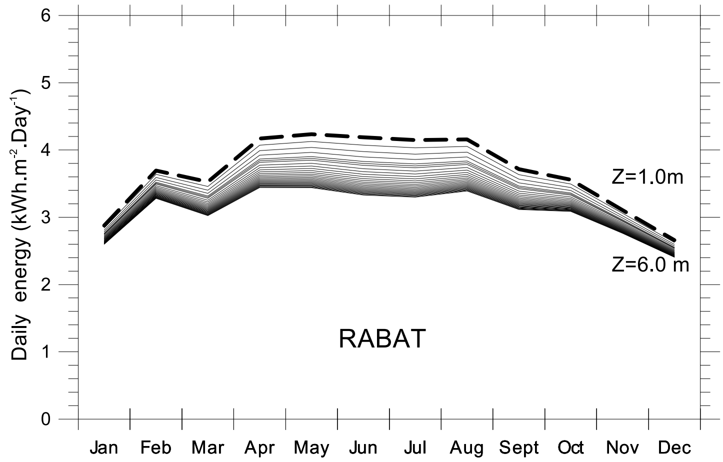

Figure 9-a

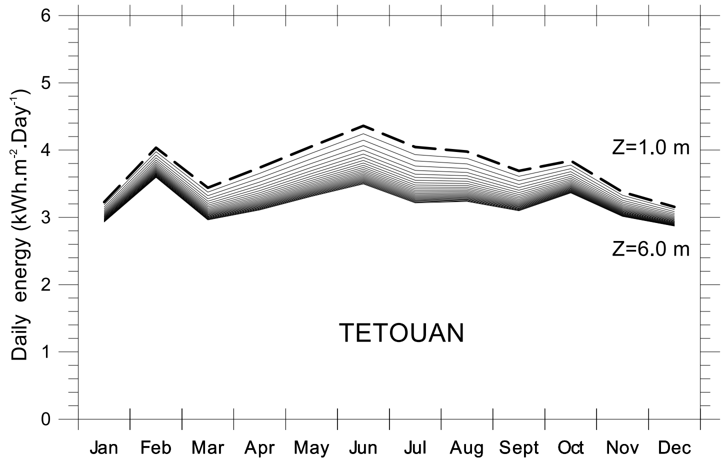

Figure 9-b

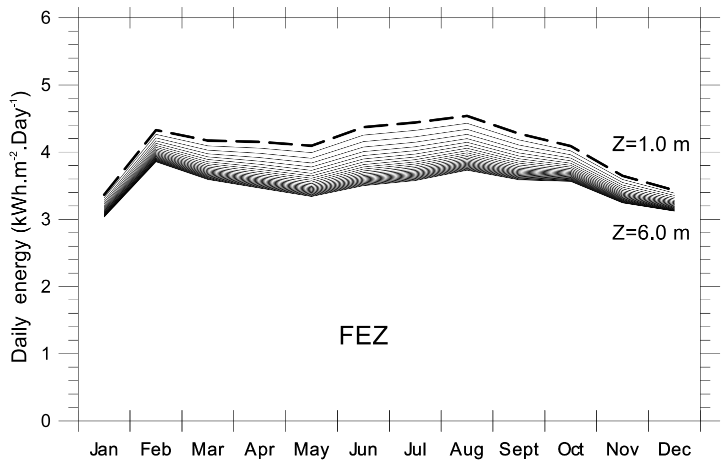

Figure 9-c

Figures 9-c Variation of the MADIE average for different values of Z.

Figures 9 indicate that the increase in the Z values leads to a systematic decrease of the MADIE average.
For the three studied sites, the change of gain, as a function of Z, is visualized by Figure 7.c. From this figure, it is found that:

- the gain variation profile is similar for all the three sites;
- for high values of Z, the decrease in gain stabilizes at around an asymptotic minimum value, with an almost negligible difference between the three sites.

Therefore, later in this study, we will be interested only to the variation along the Ox and Oy axes.

3.1.4 Variation along both Ox and Oy directions

By using the data measured for each studied site, Z is maintained at 1 m and the MADIE average for the two extreme seasons (June for the summer and December for winter) will be calculated. Figures 10 are obtained by varying progressively the values of X from 1.50 m to 16.00 m, by step of 0.25 m, and for each value of X, Y is varying from 1.2 m to 16.2 m, by an increment of 0.3 m.

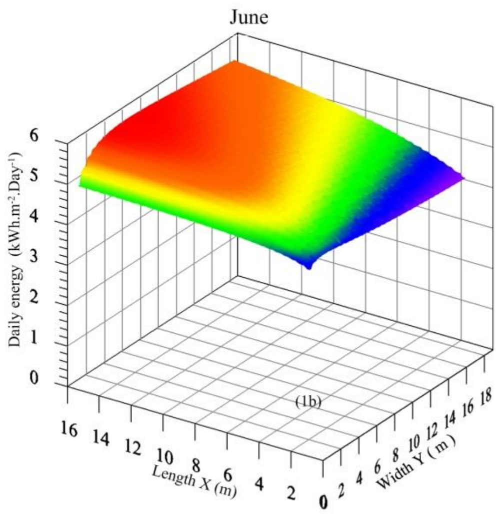

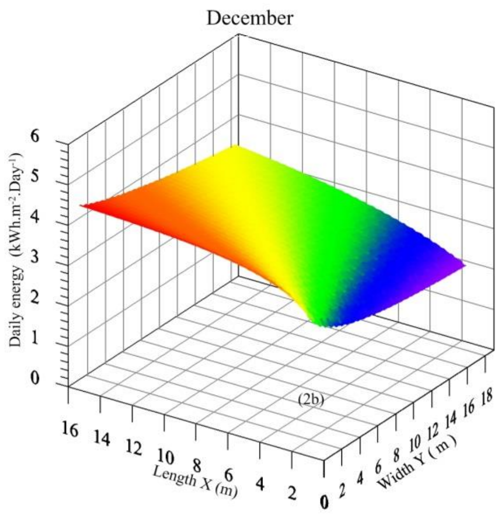

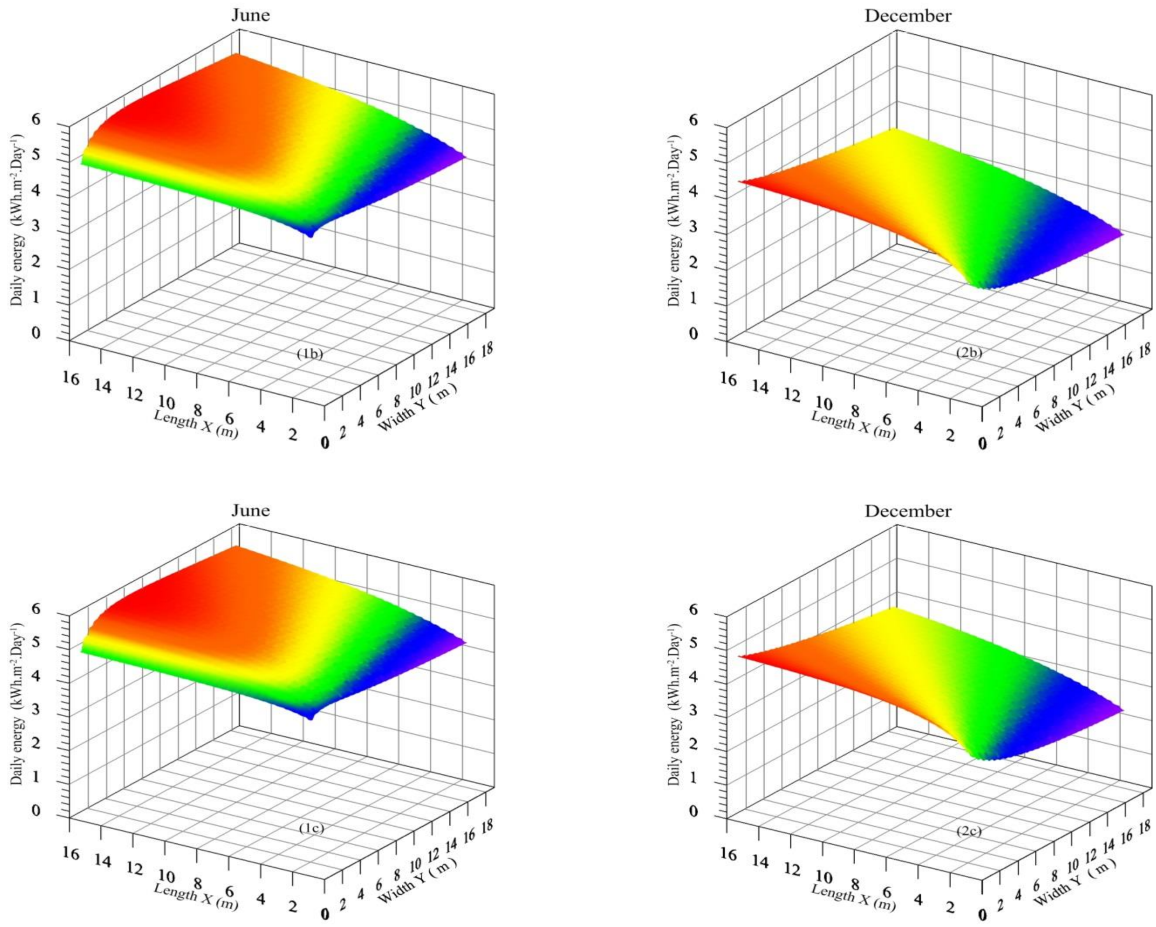

Figure 10 Variation of the MADIE average along both OX and OY directions.

These figures show that:

- during each of the two seasons (summer and winter) and for the three sites, the trends of the energy surfaces variation for the (X,Y) value pairs are respectively similar and present a curved appearance;
- energy surfaces describing the variations of X and Y in the winter (Figures 10.1.a, 10.1.b and 10.1.c) take a flat shape and differ from those illustrated during the summer which are rather softly curved (Figures 10.2.a, 10.2.b and 10.2.c);
- for the Rabat site, the energy is maximum for X = 6.0 m and Y = 16.0 m; with this value of Y, a significant increase in energy was noted for low values of X. From X = 5.5 m and up, the increase becomes less than 0.5%. This result enables us to conclude that the best pair (X,Y), corresponding to an optimum energy of 4.94 $kWh.m^{-2}.Day^{-1}$, is that for which X = 5.5 m and Y = 6.0 m.

By proceeding analogously to the sites of Fez and Tetouan, the achieved results are presented in Table 3 below.

Table 3 The best pairs (X,Y) and corresponding optimal energies for the three studied sites.

Sites	**X (m)**	**Y (m)**	**Optimal energy ($kWh.m^{-2}.Day^{-1}$)**
Rabat	5.50	6.00	4.94
Fez	5.50	6.00	5.14
Tetouan	5.75	6.00	5.12

3.1.5 Variation of Z for the optimal (X,Y) dimensions

The results obtained previously consider only the value of Z = 1.0 m. For higher values (Z = 1.0 m to 6.0 m), it was found that the daily energy profiles of the MADIE average decreases similarly in comparison with those drawn in figures 9 below. For each site, this effect is illustrated by figures 11 where the dimensions of the dryer are equal to the optimal values of X and Y.

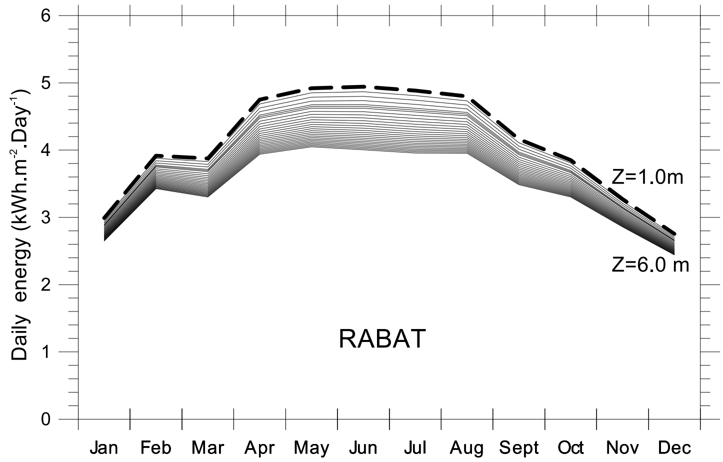

Figure 11-a

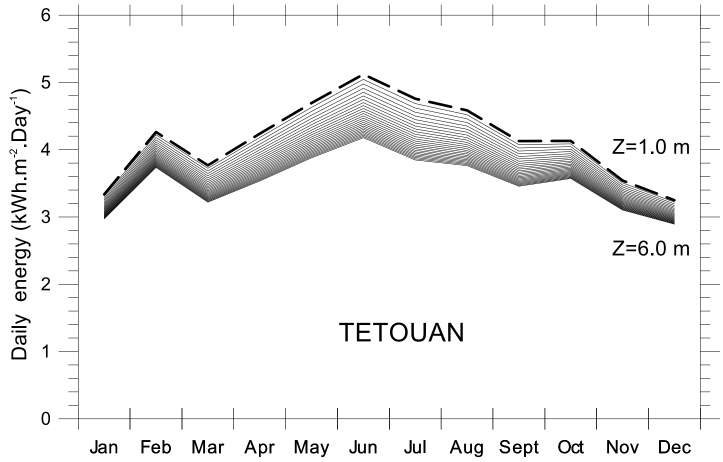

Figure 11-b

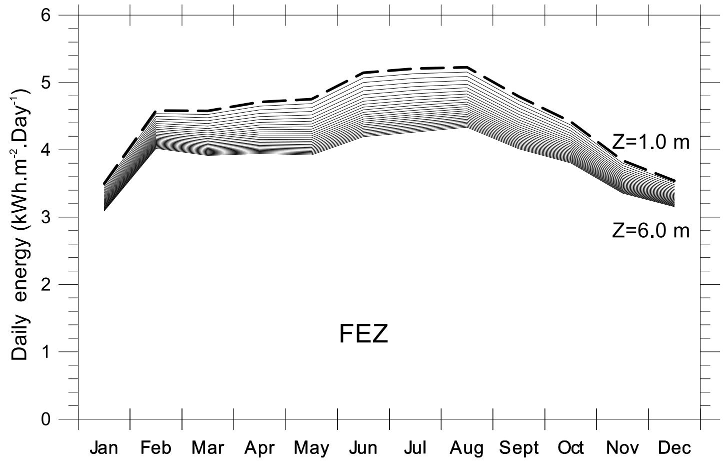

Figure 11-c

Figures 11 Variation of the MADIE average for different values of Z with optimal dimensions of X and Y.

After calculating the energy lost occurred by the variation of Z, for both standard and optimal values of (X,Y), we identified, for each site, a clear difference, particularly, from Z = 1.0 m to 5.0 m (see figure 12).

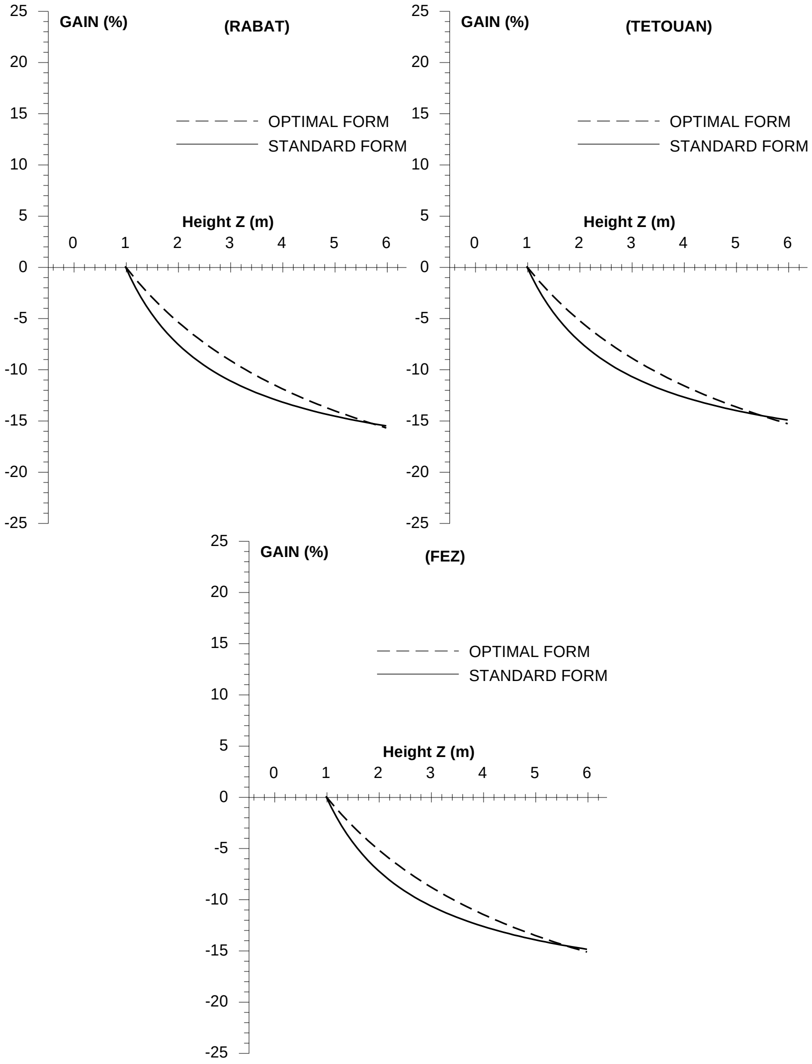

Figure 12 Energy lost occurred by the variation of Z for both standard and optimal dimensions of (X,Y).

Figure 13 represents the variation, in function of Z, of the gain difference between the (X,Y) standard and optimal dimensions and indicates that this difference reach a maximum corresponding to the optimal value of Z = 2.3 m for the three sites.

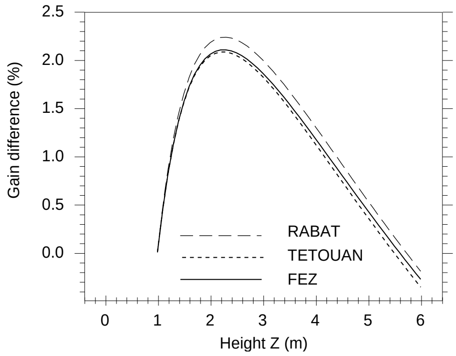

Figure 13 Variation of the gain difference between standard and optimal dimensions of (X,Y) in function of Z for the three sites.

Consequently, the functional choice of the dryer size height Z for optimal dimensions of X and Y depends uniquely on the destined use of the dryer.

4. Conclusion

In this investigation, we have discussed, for a year of measurements and for three different Moroccan climates, the impact of the variation of the dryer geometry on the incident and transmitted energy. This study was performed by taking into account the influence of the site's climatic specificity on the variation of these energies. It has led us to the following conclusions:

- compared to the received energy by the DSD standard form, the variation of X, Y and Z dimensions doesn't conduct to the same incident energy variation: increasing of X values promotes an increase in daily incident energy; increasing of Z values leads to a decrease of this energy and increasing of Y values leads to its decrease during winter, while in summer period, the trend is the same except for some values of Y;
- for the standard geometry of the dryer, the MADIE average exceeding the annual average promotes the DSD use during seven months for the Rabat and Tetouan sites and nine months for the Fez site while the MADTE average exceeding the annual average promotes its use during eight months in all sites;
- for the optimal geometry of the dryer, both the MADIE and MADTE averages exceeding the annual average promotes the DSD use during nine months for the three sites;
- for each of the three studied sites, the best pair (X,Y) corresponding to an optimal daily solar energy has been established.

References

[1] K. Kabidi, H. Samrani, M.N. Bargach and R. Tadili, 2014. "Energy performance study of a direct solar dryer installed under sub humid region", IIRE journal, Vol.9, n°.1, 8 p.

[2] Y. Jannot, 2011. ''Thermique solaire'', Ecole des Mines de Nancy, France, 80 pages.

[3] A. Boussalia, 2010. ''Contribution à l'étude de séchage solaire de produits agricoles locaux'', Mémoire présenté en vue de l'obtention du Diplôme de Magister en Génie Climatique, Alger, 119 pages.

[4] D.K. Gough, 1981. ''Timber seasoning in a solar kiln'', Technical paper, Department of Forestry, Queensland, 0155-9664, n°. 24, 6 p.

[5] R. Benkhelfellah, S. El Mokretar, R. Miri and M. Belhamel , 2005. ''Séchoirs solaires. Etude comparative de la cinétique de séchage des produits agroalimentaires dans des modèles de type direct et indirect'', 12èmes Journées Internationales de Thermique, Morocco, pp. 259-262.

[6] Ch. Perrin de Brichambaut, 1963. ‘‘Rayonnement solaire et échanges radiatifs naturels’’, Gauthier-Villards, Paris, Vol 79, 469 p.

[7] R. Tadili and M.N. Bargach, 2005. ‘‘Une méthode d’estimation du rayonnement solaire global reçu par une surface inclinée. Application aux sites marocains’’, Revue de la Société Météorologique de France, 8ème série, n° 50, pp. 46-50.

[8] J. Bahraoui-Buret, M.N. Bargach and M.L. Benkaddour, 1983. ‘‘Le Gisement Solaire Marocain’’, Laboratoire d’Energie Solaire et d’Environnement, Rabat – Maroc, 111 p.

[9] J.P. Mathieu, 1965. ‘‘Optique électromagnétique’’, Société d’Édition d’Enseignement Supérieur S.E.D.E.S., Paris, 341 p.

[10] A. Nisen, J. Deltour, J. Nijskins and S. Coutisse, 1986. ‘‘Considérations pratiques sur la transmission du rayonnement solaire et de la chaleur pour les matériaux utilisés en serres comme couverture, ombrage et écrans thermiques’’, Centre d’Étude des Économies d’Énergie en Cultures Protégées, I.R.S.I.A., Belgique, 94 p.